Available online at www.sciencedirect.com
ScienceDirect
Geochimica et Cosmochimica Acta 73 (2009) 5693–5708
Geochimica et Cosmochimica Acta
www.elsevier.com/locate/gca

Chlorine variations in the magma of Soufrière Hills Volcano, Montserrat: Insights from Cl in hornblende and melt inclusions

M.C.S. Humphreys [a,*], M. Edmonds [a], T. Christopher [b], V. Hards [c]

[a] Department of Earth Sciences, University of Cambridge, Downing Street, Cambridge CB2 3EQ, UK
[b] Montserrat Volcano Observatory, Flemmings, Montserrat, West Indies
[c] British Geological Survey, Keyworth, Nottingham NG12 5GG, UK

Received 21 January 2009; accepted in revised form 15 June 2009; available online 23 June 2009

Abstract

The Soufrière Hills Volcano in Montserrat erupts a Cl-rich, porphyritic andesite. HCl degassing accompanies eruption and is dependent on the growth rate of the lava dome. The magma contains hornblende phenocrysts that show repetitive zoning in most elements, including Cl. On the basis of the zoning data, (Cl/OH) ratios in the melt, calculated from partitioning data, increase rimward through each zone, indicating that the phenocrysts formed under conditions of varying $(Cl/OH)_m$. An empirical relationship between A-site occupancy in the hornblende and temperature implies that crystallisation of each zone is also accompanied by increasing temperature. Each zone ends at a resorption horizon, and crystallisation recommences at lower temperature and $(Cl/OH)_m$. Melt inclusion H_2O and Cl contents for the 8th January 2007 explosive eruption can be explained by closed-system degassing with $D_{Cl}^{fl\text{-}m}$ between 5 and 30, or by open-system degassing accompanied by a small amount of crystallisation. However, neither simple closed-system degassing nor convective circulation of magma can explain the positive correlation of $(Cl/OH)_m$ with temperature. We suggest that the zoning can be caused by accumulation of CO_2-rich vapour in the andesite, probably as a result of mafic magma injection into the chamber. Decreasing H_2O fugacity and/or increasing Cl_m result in increasing $(Cl/OH)_m$ while heat transferred with the volatiles causes the rise in temperature. Intermittently, the accumulated fluid is lost to the surface, possibly as a result of renewed eruptive activity. This model requires the CO_2-rich fluid to be decoupled from the magma, consistent with previous observations of continuous CO_2 emissions at the surface.

1. INTRODUCTION

The behaviour of magmatic volatiles is one of the primary influences on the eruptive activity of arc volcanoes. Closed-system degassing leads to the build-up of gas pressure beneath the vent and can result in explosive behaviour. In contrast, open-system degassing can cause almost complete degassing of the magma and results in the build-up of a highly viscous lava dome during effusive eruptions. Despite its much lower abundance than some volatile species (e.g. H_2O, CO_2; Wallace, 2005), Cl is an important volatile and a good source of information about the degassing regime. It is incompatible in the melt and is partitioned strongly into an exsolved vapour phase (e.g. Kilinc and Burnham, 1972; Webster and Holloway, 1988; Webster, 1992); thus it can help to constrain the nature and extent of magmatic degassing. Cl is a particularly significant volatile component in arc systems; Cl contents of evolved arc magmas are high (typically 1500–3000 ppm, Wallace, 2005). The Soufrière Hills Volcano, Montserrat has particularly high Cl concentrations in both the magma and emitted gas phase (e.g. Hammouya et al., 1998; Oppenheimer et al., 1998; Edmonds et al., 2001, 2002; Harford et al., 2003). Higher Cl concentrations have been reported only for Augustine Volcano (Symonds et al., 1990). Combined

* Corresponding author. Tel.: +44 (0) 1223 333433; fax +44 (0) 1223 333450.
E-mail address: mcsh2@cam.ac.uk (M.C.S. Humphreys).

0016-7037/$ - see front matter © 2009 Elsevier Ltd. All rights reserved.
doi:10.1016/j.gca.2009.06.014

use of melt inclusion and gas emissions data has previously allowed interpretation of Cl degassing processes. For Soufrière Hills Volcano, experimental and petrological studies have previously determined that surface HCl emissions are the result of syn-eruptive degassing of Cl from the andesite (Edmonds et al., 2001; Signorelli and Carroll, 2001; Edmonds et al., 2002; Villemant et al., 2008) as it undergoes decompression crystallisation (e.g. Sparks et al., 2000; Harford et al., 2003; Couch et al., 2003). In contrast, SO_2 is thought to originate in the mafic magma; SO_2 emissions are therefore related to permeability of the magma system and changes in SO_2 supply from the mafic magma at depth (e.g. Young et al., 1998; Edmonds et al., 2001; Oppenheimer et al., 2002). The main source of CO_2 emissions is also thought to be the deep mafic magma (Edmonds et al., in review).

Cl can also be taken into some phenocryst phases (e.g. hornblende, biotite) along with other volatiles (e.g. F, Li, Rowe et al., 2008). Hornblende is a useful mineral for tracking magma conditions, because its composition responds to external parameters including oxygen fugacity (Scaillet and Evans, 1999), temperature and pressure (e.g. Holland and Blundy, 1994; Rutherford and Devine, 2003; Johnson and Rutherford, 1989). Soufrière Hills Volcano typically erupts a porphyritic andesite with hornblende phenocrysts that show wide cyclic or repetitive zoning. Similar, but finer-scale zoning has been observed in the Unzen dacite and was interpreted as the result of volatile transfer from mafic material ponding near the base of the chamber, and consequent degassing and crystallisation of the andesite (Sato et al., 2005). Rutherford and Devine (2003) studied zoning in hornblende phenocrysts erupted at Soufrière Hills Volcano during 1995–2002, and concluded that it represented major-element change associated with magma mixing; however no Cl data were available. Magma mixing is an important process at Soufrière Hills Volcano (e.g. Murphy et al., 2000; Couch et al., 2001; Devine et al., 2003), and recent work has shown that phenocrystic amphiboles and those from mafic inclusions can be distinguished on the basis of minor-element compositional differences (Humphreys et al., 2009).

Here, we report new measurements of H_2O and Cl in matrix glass and plagioclase-hosted melt inclusions from a small explosive event at Soufrière Hills Volcano in January 2007, as well as major- and minor-element data from zoned hornblendes erupted between 2001 and 2007. These data are combined with the H_2O/Cl ratio of gases emitted at the surface, as well as Cl concentrations from the zoned hornblendes. We present a quantitative degassing model for the recently erupted magma, and interpret the hornblende zoning as a result of transfer of hot, CO_2-rich vapour from mafic material into the andesite.

2. SAMPLES AND METHODS

This study focuses on material from the second and third phases of dome growth at Soufrière Hills Volcano, erupted between July 2001 and January 2007. 14 samples were studied, including 13 samples of hornblende–plagioclase andesite and one macroscopic mafic inclusion (see Table 1 of Humphreys et al., 2009 for samples and modal compositions). The samples include dome rocks and pumiceous pyroclastic flow material.

2.1. Electron probe microanalysis (EPMA)

Mineral compositions were analysed using a Cameca SX-100 5-spectrometer electron microprobe at the University of Cambridge. Major elements were analysed with a 15 kV, 10 nA beam; a 15 kV, 100 nA beam was used for minor elements. The beam was focused to a 2 μm spot. Glasses were analysed using a 15 μm, 15 kV beam with 2–4 nA beam current for major elements and 10 nA beam for minor elements. Na and Si were analysed first with short counting times in order to reduce migration of alkalis (following Devine et al., 1995; Blundy and Cashman, 2005; Humphreys et al., 2006). Typical peak counting times were 20 s for major elements and 30 s for minor elements.

2.2. Secondary ion mass spectrometry (SIMS)

Plagioclase crystals containing melt inclusions were mounted in resin and prepared using diamond polishing techniques to reveal the inclusions. Following major-element analysis, the grain mounts were coated in gold for SIMS analysis. Matrix glasses and melt inclusions in plagioclase were analysed for $^{1}H^{+}$, $^{7}Li^{+}$, $^{23}Na^{+}$, $^{35}Cl^{+}$ and $^{42}Ca^{+}$ using a Cameca ims-4f ion microprobe at the University of Edinburgh, controlled by Charles Evans and Associates PXT interface and software. A 5 nA primary beam of O^{-} ions was accelerated onto the sample surface with a net impact energy of 14.5 keV. The surface was cleaned using a 2 min pre-sputter with the beam rastered over a 10 μm square area. The beam size was approximately 14×17 μm. Counts were collected over 10 cycles. Mass 0.7 was used to monitor the background count rate of the electron multiplier detector. The mass spectrometer was calibrated for the secondary ions prior to each analysis. ^{30}Si was used as the internal standard, and the NIST standard SRM610 was used as the primary calibration standard. For smaller inclusions, an aperture was introduced that effectively reduced the beam current to ~1.5 nA, and the beam size to approximately 10×13 μm. This gave slightly higher analytical uncertainties, of $\leqslant$4% relative for Cl and $\leqslant$1% relative for Li (compared with $\leqslant$2% and $\leqslant$0.6% relative respectively for the larger beam). H_2O contents were calculated from a daily working curve of H/Si vs. H_2O (Blundy and Cashman, 2005), which gives a straight line with R^2 0.98 or better for a set of well-characterised standard glasses, following the procedure described in Humphreys et al. (2006) and Blundy and Cashman (2005). This method gave typical errors in determining H_2O of 5–15% relative. For Cl and F, two standards were used with 1550 ppm Cl and 2230 ppm F, and 530 ppm Cl, 770 ppm F, respectively.

Major-element analyses that had analytical totals outside the range 98–102% (when including H_2O measured by SIMS) were discarded, as were those with poor correlation between H_2O from SIMS and volatiles by difference

Table 1
Volatile contents of melt inclusions and matrix glasses as analysed by SIMS. H_2O speciation is calculated using Zhang (1999), assuming a temperature of 850 °C (see text). $(Cl/OH)_m$ is calculated from Cl normalised to molar mass fraction following Sato et al. (2005). Pressure is calculated assuming $pH_2O = P_{tot}$ (Newman and Lowenstern, 2002). Analyses followed by lowercase 's' were analysed using the small SIMS aperture in order to reduce SIMS beam size (see text for details). Electronic annex: Hornblende zoning profiles.

Analysis		H_2O wt%	± (wt%)	Cl wt%	Li ppm	$[H_2Ot]$	$[H_2Om]$	[OH]	Norm Cl	Cl/OH m	P MPa (no CO_2)
MVO1524b_42	Melt inclusion	1.14	0.10	0.226	7.0	0.020	0.002	0.037	0.0020	0.0536	11
MVO1524b_112	Melt inclusion	3.37	0.05	0.290	18.7	0.059	0.014	0.091	0.0025	0.0277	78
MVO1524b_142	Melt inclusion	4.28	0.08	0.396	68.3	0.075	0.020	0.108	0.0034	0.0317	118
MVO1524b_151	Melt inclusion	1.79	0.03	0.298	34.6	0.032	0.005	0.054	0.0026	0.0477	26
MVO1524d_22	Melt inclusion	4.15	0.12	0.461	22.5	0.072	0.019	0.106	0.0040	0.0378	112
MVO1524d_31	Melt inclusion	5.16	0.15	0.359	31.3	0.089	0.027	0.124	0.0031	0.0251	161
MVO1524d_41s	Melt inclusion	6.24	0.91	0.426	69.2	0.107	0.037	0.141	0.0037	0.0262	216
MVO1524d_81s	Melt inclusion	3.17	0.12	0.367	28.8	0.056	0.013	0.086	0.0032	0.0368	71
MVO1524d_91	Melt inclusion	2.06	0.07	0.272	21.8	0.037	0.006	0.061	0.0024	0.0386	33
MVO1524d_93s	Melt inclusion	2.03	0.21	0.206	24.8	0.036	0.006	0.060	0.0018	0.0296	32
MVO1524d_101s	Melt inclusion	5.07	0.38	0.356	42.9	0.088	0.027	0.122	0.0031	0.0252	156
MVO1524d_142s	Melt inclusion	5.72	0.24	0.437	36.9	0.099	0.032	0.133	0.0038	0.0285	189
MVO1524d_151	Melt inclusion	5.07	0.39	0.437	25.1	0.088	0.027	0.122	0.0038	0.0310	156
MVO1524d_152	Melt inclusion	4.96	0.25	0.430	23.7	0.086	0.026	0.120	0.0037	0.0310	151
MVO1524d_153s	Melt inclusion	5.50	0.81	0.394	32.2	0.095	0.030	0.129	0.0034	0.0264	178
MVO1524d_162	Melt inclusion	2.24	0.18	0.309	23.5	0.040	0.007	0.065	0.0027	0.0409	38
MVO1524d_61	Matrix glass	0.18	0.01	0.130	16.7	0.003	0.000	0.006	0.0012	0.1876	0.3
MVO1524d_62	Matrix glass	0.33	0.01	0.159	17.7	0.006	0.000	0.011	0.0015	0.1274	0.9
MVO1524d_64s	Matrix glass	0.17	0.00	0.187	15.8	0.003	0.000	0.006	0.0017	0.2866	0.3

(VBD) from the electron microprobe. The degree of correlation between Ca(SIMS) and CaO (EPMA) and between Cl (SIMS) and Cl (EPMA) was also checked, for indications that the analyses might be contaminated by the host plagioclase. Post-entrapment crystallisation, which can be recognised on back-scattered electron images as a thin rind of plagioclase deposited on the walls of the inclusion, was absent in these inclusions.

3. GEOLOGICAL BACKGROUND

The Soufrière Hills Volcano erupts porphyritic andesite with abundant basaltic to basaltic andesite inclusions. The phenocryst assemblage in the andesite is hornblende + plagioclase + orthopyroxene + quartz + magnetite ± ilmenite, although quartz is commonly resorbed and may only be stable in the cooler margins of the magma reservoir (Barclay et al., 1998; Devine et al., 2003; Humphreys et al., 2009). Inclusions of plagioclase in hornblende are common, indicating co-crystallisation. Microphenocrysts of apatite are commonly observed. The groundmass comprises plagioclase + clinopyroxene + orthopyroxene + Fe–Ti oxides; some of these microlites originated in mafic inclusions that disaggregated during ascent (Humphreys et al., 2009). Dome rocks typically show vesicular textures filled in with cristobalite. Mafic inclusions are vesicular, with elongate crystals of plagioclase + clinopyroxene + orthopyroxene + Fe–Ti oxides. The larger inclusions tend to contain hornblende instead of clinopyroxene (Murphy et al., 2000).

Phenocryst zoning has been described in detail by several authors (e.g. Murphy et al., 2000; Rutherford and Devine, 2003; Zellmer et al., 2003; Humphreys et al., 2009). There is abundant evidence for chemical disequilibrium in plagioclase, orthopyroxene and quartz, with textures attributed either to heating or interaction with hotter, mafic magma (e.g. Murphy et al., 2000; Devine et al., 2003; Humphreys et al., 2009). Hornblende also shows different reaction and breakdown textures (Fig. 1). Where they are fresh, hornblende phenocrysts show a relatively homogeneous core and a zoned rim (Fig. 1a). Each new zone boundary is sharp, and associated with slight rounding or resorption. Interaction with hotter, more mafic magma causes crystallisation of a coarse-grained, clinopyroxene-rich reaction rim, with the new crystals typically aligned parallel to the *c*-axis of the original grain (Rutherford and Devine, 2003; Humphreys et al., 2009; Fig. 1b). Resorption and the formation of fine-grained decompression breakdown rims may occur if ascent is slow (e.g. Rutherford and Hill, 1993; Rutherford and Devine, 2003; Browne and Gardner, 2006; Fig. 1c). Finally, oxidation during shallow storage in the dome causes replacement of the whole grain by a fine-grained aggregate dominated by opaque minerals (e.g. Garcia and Jacobson, 1979; Murphy et al., 2000; Plechov et al., 2008; Fig. 1d).

Pre-eruptive storage conditions for the andesite have been determined from experimental phase petrology and thermobarometry, and are relatively oxidising (NNO + 0.5) with pressures of at least 115–130 MPa (Barclay et al., 1998). Temperatures were ~800–840 °C with local heating to ~900 °C or more due to injection of mafic magma (Barclay et al., 1998; Devine et al., 1998; Murphy et al., 2000; Devine et al., 2003; Humphreys et al., 2009). Glassy crystal clots give cooler temperatures and more oxidising conditions (780 °C, NNO + 1.5) that may represent conditions on the margin of the storage region.

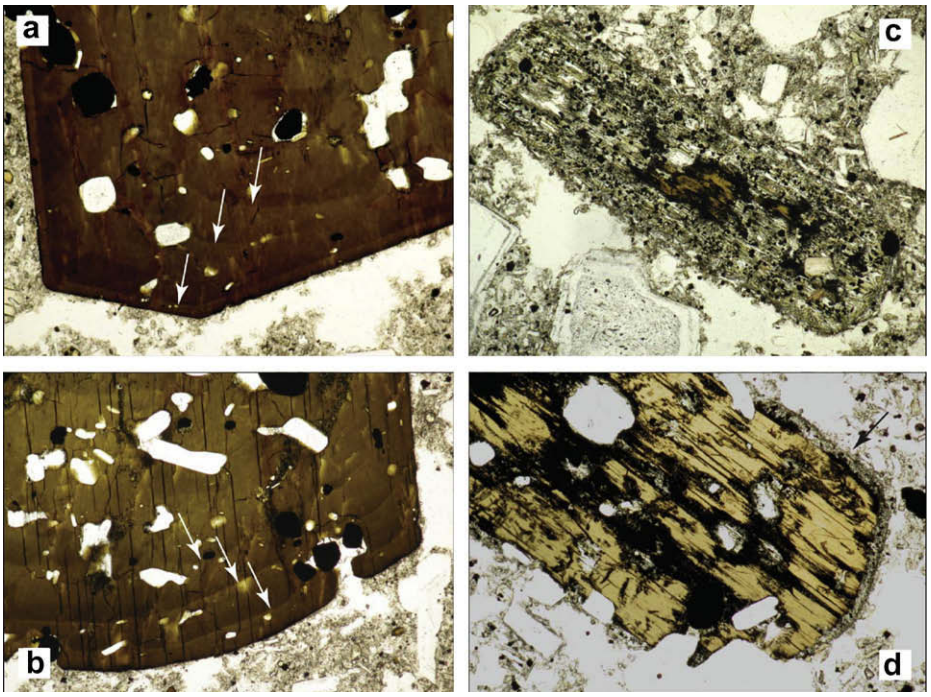

Fig. 1. Typical hornblende textures from the Soufrière Hills andesite. (a) and (b) Oscillatory zoned margins of euhedral hornblende phenocrysts. Each zone (white arrow) has a sharp onset and is associated with slight rounding or resorption. (c) Coarse-grained, clinopyroxene-rich reaction rim formed through interaction with more mafic magma. (d) Hornblende with narrow, fine-grained decompression break-down rim. The grains in (c) and (d) are also partially opacitised (blackened regions).

4. HORNBLENDE COMPOSITIONS

Amphibole compositions are described by Humphreys et al. (2009) and summarised here. Structural formulae were calculated on the basis of 23 oxygen atoms, following Schumacher (1997), and assuming a stoichiometric number of anions (OH + Cl + F = 2). The amphiboles range from Mg-hornblende to Mg-hastingsite (Leake et al., 1997). The compositions of phenocrysts from the andesite reflect control by the edenite substitution ($Si^T + [\ ] = Al^T + (Na + K)^A$) but indicate little effect of the Tschermak substitutions $Si^T + Mg^{vi} = Al^T + Al^{vi}$ and $Si^T + Mn^{vi} = Al^T + Ti^{vi}$. Following Bachmann and Dungan (2002), approximately 50% of the phenocryst compositional variation can be explained by the edenite exchange, ~20% by the Ti-Tschermak exchange and ~15–20% by the Tschermak exchange. Mafic amphiboles, microphenocrysts and microlites cover a much wider range of compositions than the phenocrysts. In particular they show higher $(Na + K)^A$ and Al^T (Fig. 2a) and also show a good correlation between Al^T and Al^{vi}. In contrast to the phenocrysts, only ~20% of the compositional variation can be attributed to the edenite exchange. However, the good correlation between Al^T and Al^{vi} in microlites, microphenocrysts and mafic amphiboles cannot be explained by the Tschermak substitution, because Al^T lacks the good negative correlation with Mg^{vi} shown by the phenocrysts (Fig. 2b). The mafic amphiboles, microlites and microphenocrysts also have higher Mg# (calculated as Mg/(Mg + Fe)) than the phenocrysts. Within each textural group, there are no systematic differences in hornblende composition between samples. However, hornblende phenocrysts from the andesite can easily be distinguished from amphiboles that originated in the mafic inclusions, on the basis of their minor-element compositions.

4.1. Chlorine contents of hornblendes

In phenocrysts in the andesite, typical chlorine concentrations range from 0.08 wt% to 0.17 wt% Cl, with a few analyses showing very high Cl contents of >0.2 wt%. Cl concentration decreases with increasing Mg# (Fig. 3). This reflects in part the decrease in the partition coefficient for chlorine with decreasing Fe content, which occurs because the large Cl ion can substitute more easily for Fe^{2+} than for Mg^{2+} (Volfinger et al., 1985; Oberti et al., 1993; Sato et al., 2005). F concentrations are low, typically 0.04–0.06 wt%, show no systematic variation with Mg# or other compositional parameters, and are not considered further. The correlation between Mg# and Cl is qualitatively consistent with hornblende compositions from Unzen Volcano (Sato et al., 2005); however hornblende from Soufrière Hills Volcano has much higher Cl contents than in comparable systems (Fig. 3; e.g. Unzen, Japan, Sato et al., 1999, 2005; Pinatubo, Philippines, Matthews et al., 1992; Mount St. Helens, USA, Rowe et al., 2008).

Amphiboles from the mafic inclusions have much lower Cl contents than the phenocrysts, typically <0.03 wt% Cl (Fig. 3). The mafic amphiboles also have significantly higher Mg# than the phenocrysts (Mg# 77–88 cf. Mg# 61–70), and fall on a shallower Cl–Mg# gradient (Fig. 3).

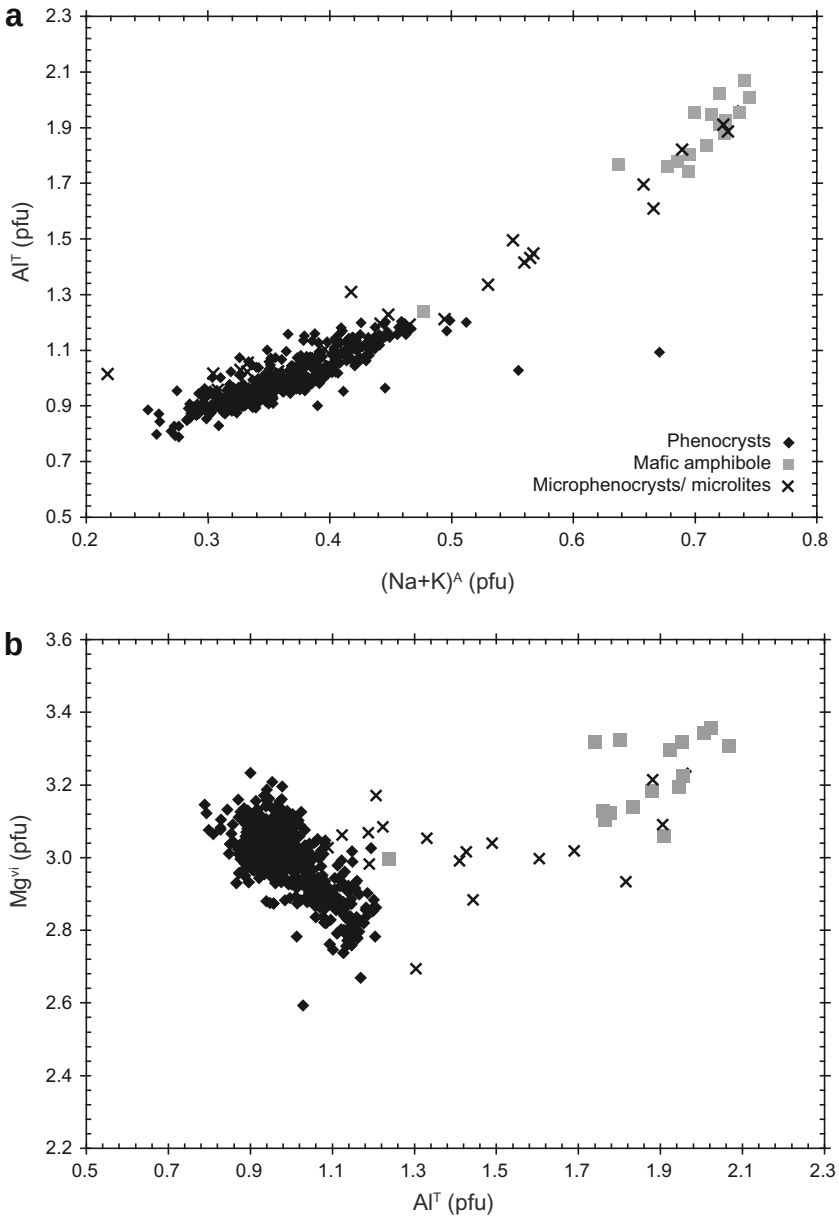

Fig. 2. Amphibole compositions from Soufrière Hills, after Humphreys et al. (2009). (a) Phenocrysts and mafic amphiboles both show a good correlation of Al^T with $(Na + K)^A$, but mafic amphiboles have higher Al^T and $(Na + K)^A$. (b) Phenocrysts show a negative correlation of Mg^{vi} with Al^T, while mafic amphibole compositions are more scattered and lack the good negative correlation. This can be ascribed to reduced silica activity in a more mafic melt (Sato et al., 2005).

4.2. Phenocryst traverses

Compositional traverses were obtained across the margins of several phenocrysts with clear repetitive zonation (electronic annex). Each zone is defined by a sharp increase in Mg and Si, and decrease in Al, Na, K, Cl, Fe and Ti. This is followed by a rimward recovery towards the original values (Fig. 4). The traverses show the same correlations between minor elements as the main phenocryst population, including a good negative correlation between Mg^{vi} and Al^T. This is significantly different to that seen for the mafic amphiboles (Fig. 2) and indicates that the zoning is not produced by mixing with mafic material.

5. MELT INCLUSIONS AND MATRIX GLASSES

Matrix glasses and quartz- and plagioclase-hosted melt inclusions from previous phases of dome growth at Soufrière Hills Volcano have been reported by several authors (Barclay et al., 1998; Edmonds et al., 2001; Harford et al., 2003; Buckley et al., 2006; Rutherford and Devine, 2003). We studied the matrix glass and plagioclase-hosted melt

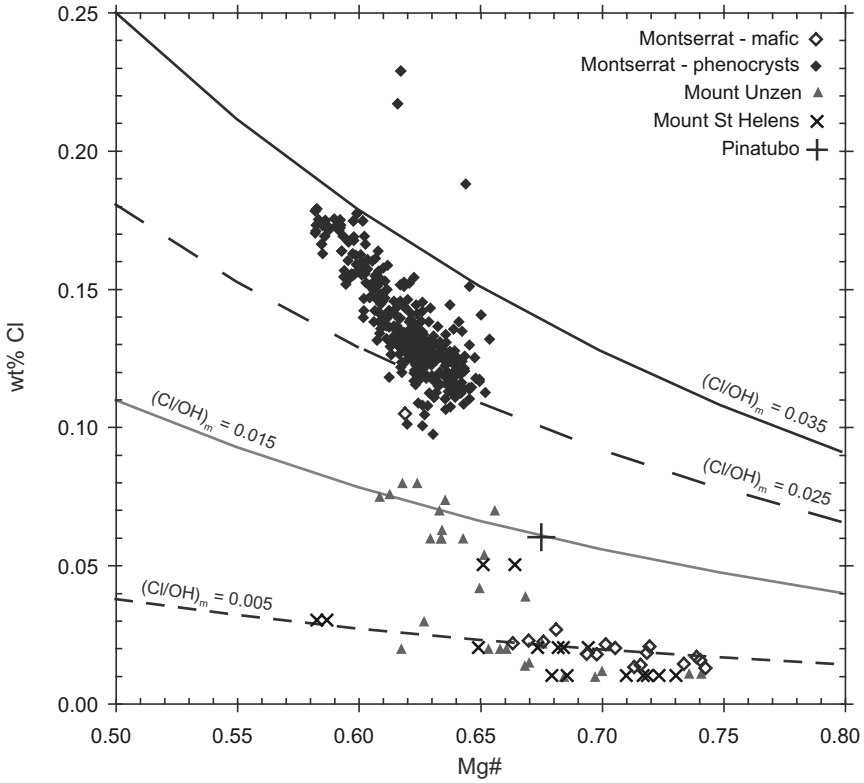

Fig. 3. Cl content and Mg# of amphiboles from Montserrat, with data from other arc volcanoes for comparison. Lines indicate amphibole compositions calculated for constant temperature and (Cl/OH) ratio in the melt (see text, later, for details of calculation). Data sources: Unzen, Japan: Sato et al. (1999, 2005); Mount St. Helens, USA: Rowe et al. (2008); Mt Pinatubo, Philippines: Matthews et al. (1992).

inclusions in two samples of a pumiceous pyroclastic flow deposit that was emplaced into the Belham Valley on 8th January 2007. The flow was emplaced during an explosive event that produced a number of minor pyroclastic flows accompanied by ash venting. Hornblende phenocrysts from the same samples were also studied. The melt inclusions are dominantly rhyolitic (69–79 wt% SiO_2 on an anhydrous basis) and similar in composition to previously reported analyses. Their compositions will be described fully in a separate study. The inclusions were analysed by SIMS for volatile elements including H_2O, Li and Cl (Table 1). They contain up to 6.2 wt% H_2O, while matrix glasses have up to 0.33 wt% H_2O. Cl and Li contents are high and variable, and show a positive correlation with H_2O contents (Fig. 5). The H_2O contents recorded are much higher than previously observed in melt inclusions from Montserrat (4.5 wt% H_2O, Barclay et al., 1998) and indicate magma storage at high pressures (at least 220 MPa; higher if there is CO_2 in the system; Newman and Lowenstern, 2002). Measured Cl concentrations are very high compared with similar volcanic systems worldwide (Fig. 5a) but are similar to those previously reported for the Soufrière Hills Volcano (e.g. Devine et al., 1998; Edmonds et al., 2001, 2002). The melt inclusions contain 1500–4500 ppm Cl and 20–70 ppm Li, while matrix glasses have much lower concentrations (1200–1600 ppm Cl and 11–18 ppm Li). The Li concentrations are typical of other silicic arc volcanoes (Fig. 5b).

6. Cl/OH PARTITIONING BETWEEN HORNBLENDE AND MELT

Zoning of Cl in hornblende may be related to changes in the major-element composition of the amphibole, the distribution coefficient, or the melt Cl/OH ratio. The distribution coefficient for Cl and OH between hornblende and melt, K_D, depends on the Mg# of the hornblende and the temperature (Sato et al., 2005):

$$K_D = \frac{(\mathrm{Cl/OH})^{hb}}{(\mathrm{Cl/OH})_m} = \exp[8.62 - 3.46\mathrm{Mg\#} - 0.0062T] \qquad (1)$$

K_D decreases as Mg# increases and as temperature decreases; the primary control on K_D is the major-element composition of the hornblende (Sato et al., 2005). However, an estimate of T is required to make an accurate assessment of K_D.

6.1. Temperature constraints

Experimental studies have shown that the Al^T and $(Na + K)^A$ contents of hornblende are dependent on temperature (e.g. Scaillet and Evans, 1999; Rutherford and Devine, 2003; Costa et al., 2004). The Al^T-$(Na + K)^A$ correlation is very good for the Soufrière Hills hornblende data ($R^2 = 0.85$, see Fig. 2) which indicates that temperature changes are important. In order to quantify the

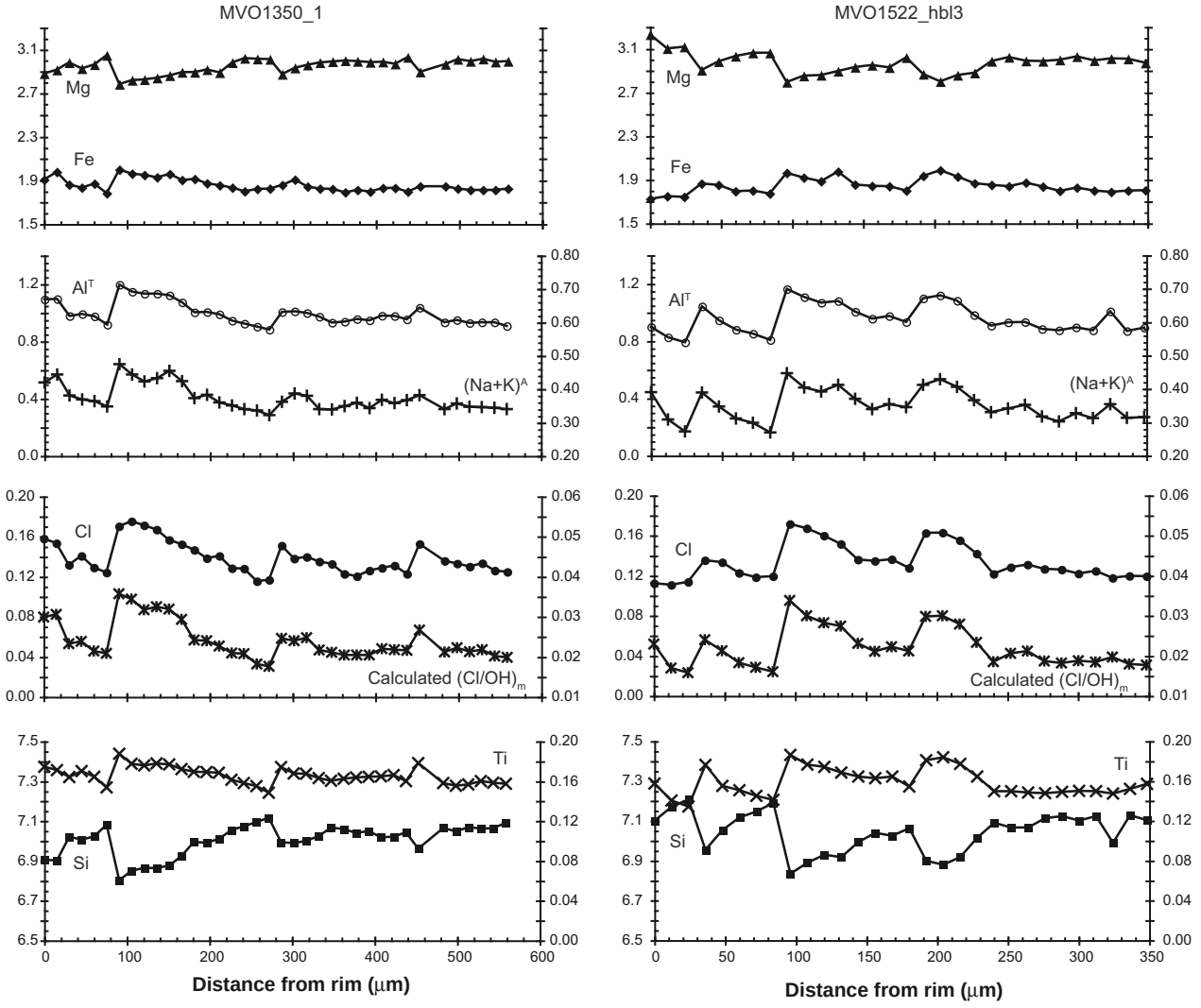

Fig. 4. Two examples of oscillatory zoning profiles from hornblende phenocrysts. Cations are plotted per formula unit. $(Cl/OH)_m$ is calculated from (Cl/OH) in hornblende (see text for details).

temperature effects on K_D, we analysed 41 plagioclase–hornblende inclusion pairs, and obtained T estimates using the hornblende–plagioclase thermometer (Holland and Blundy, 1994). The calculated temperatures range from 777 °C to 867 °C, consistent with previous estimates (e.g. Murphy et al., 2000). Compositional data from the host hornblende phenocrysts show a positive relationship between $(Na + K)^A$ and temperature (Fig. 6):

$$T = 479.8\ (Na + K)^A + 643.5\ R^2 = 0.63 \quad (2)$$

The uncertainty of the hornblende–plagioclase thermometer is approximately 35–40 °C (Holland and Blundy, 1994). Of the calculated hornblende–plagioclase temperatures, 95% lie within ±24 °C of the temperatures calculated on the basis of hornblende $(Na + K)^A$ using equation [2].

Applying equation [2] to the phenocryst traverses produces a range of temperatures from 767–872 °C, consistent with previous estimates of the initial storage conditions in the Soufrière Hills magma (e.g. Barclay et al., 1998; Murphy et al., 2000; Devine et al., 2003). These temperatures are also consistent with temperatures estimated from orthopyroxene core compositions, which are typically ~850 °C but range from 785 °C to 938 °C (Murphy et al., 2000; Humphreys et al., 2009). Using equation [2], any individual hornblende traverse typically records a temperature range of ~70 °C, the largest variation being 90 °C. The compositional change at the beginning of each zone is equivalent to a temperature decrease of up to ~60 °C.

6.2. Calculating $(Cl/OH)_{hb}$ and $(Cl/OH)_m$

Assuming a stoichiometric number of anions (OH + Cl + F = 2), we used equation [1], combined with the temperature estimated from $(Na + K)^A$ and Mg# from EPMA, to calculate K_D, and thus $(Cl/OH)_m$, at every point in the compositional traverses. This allows us to assess how much of the Cl zoning is due to changes in K_D, and how much is related to real changes in melt composition. Using the same

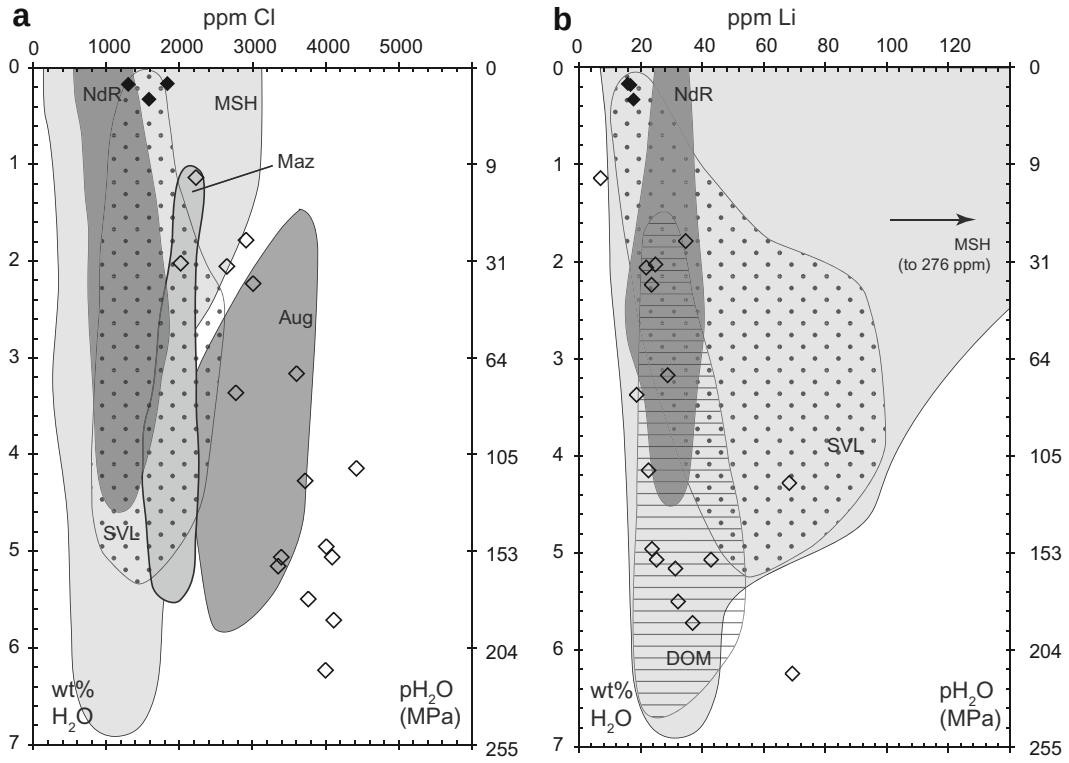

Fig. 5. Left: H_2O and Cl contents of melt inclusions from Soufrière Hills Volcano, Montserrat, as determined by SIMS. Cl decreases with H_2O, consistent with a $D_{Cl}^{fl\text{-}m} > 1$. Pressure scale is calculated for $pH_2O = P_{tot}$ at 850 °C (Newman and Lowenstern, 2002). Right: H_2O and Li contents of melt inclusions; Li decreases with decreasing H_2O, indicating that it is also partitioned into the vapour phase. Open diamonds are melt inclusions, black diamonds are matrix glass compositions. Errors are typically better than 10% relative for H_2O (see Table 1) and approximately 1% relative for Li. Values from other silicic systems are shown for comparison. MSH, Mount St. Helens (Blundy et al., 2008); Aug, augustine (Roman et al., 2006); Maz, Mount Mazama (Bacon et al., 1992); SVL, Shiveluch (Humphreys et al., 2008); NdR, Nevado del Ruiz (Stix et al., 2003); DOM, Dominica (Gurenko et al., 2005).

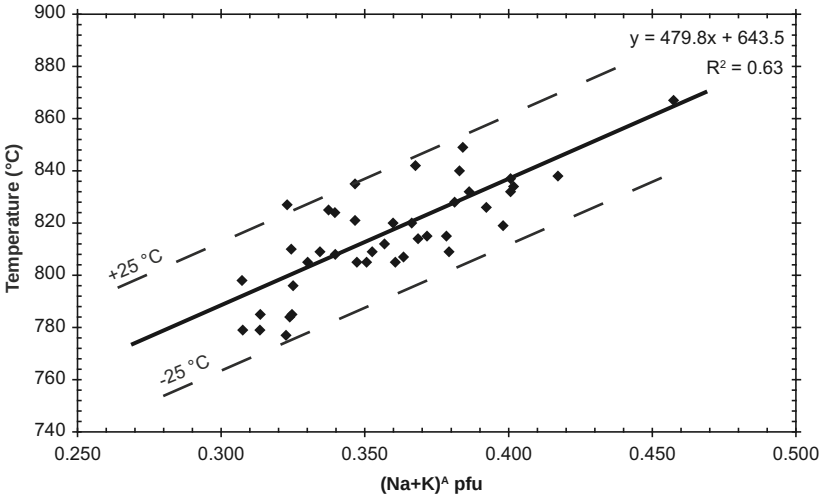

Fig. 6. Hornblende $(Na+K)^A$ *vs* temperature calculated from co-existing hornblende–plagioclase pairs, using thermometer 'B' from Holland and Blundy (1994). The uncertainty on the thermometer is quoted as ±35 °C (Holland and Blundy, 1994); 95% of the points lie within 25 °C (dashed lines) of the best-fit curve. The average absolute deviation of calculated from known temperatures is 9.8 °C.

approach, contours of Cl–Mg# in hornblende were constructed for constant $(Cl/OH)_m$ and temperature (Fig. 3). Values of $(Cl/OH)_m$ calculated in this way for the phenocrysts range from 0.015–0.037 (average = 0.024,

$1\sigma = 0.0048$, $n = 324$). In contrast, mafic inclusion hornblende gives $(Cl/OH)_m$ in the range 0.0068–0.0128 (average = 0.0095, $1\sigma = 0.0016$, $n = 15$). In other words, the mafic hornblendes crystallised under conditions of low, but constant $(Cl/OH)_m$, while the phenocrysts crystallised from a melt that experienced strong changes in $(Cl/OH)_m$ (Fig. 3). In a typical traverse of a zoned hornblende crystal, each new zone is associated with a $(Cl/OH)_m$ decrease of ~30% relative (typically an absolute decrease of 0.01–0.015). Thus crystallisation of each new hornblende zone is associated with a decrease in temperature and in the Cl/OH ratio of the melt.

$(Cl/OH)_m$ was also calculated for the melt inclusions and matrix glasses following Sato et al. (2005). The expressions of Zhang (1999), combined with the temperature-dependent equilibrium constant for H_2O speciation (Nowak and Behrens, 2001, described as "K_{ws}" in Sato et al., 2005), were used to calculated the mole fractions $[H_2O_m]$ and [OH], given the total H_2O concentrations analysed by SIMS.

Values of $(Cl/OH)_m$ calculated from the melt inclusions are consistently low, ranging from 0.020 to 0.053 with one outlier at 0.221. Matrix glasses have much higher $(Cl/OH)_m$, 0.127–0.281. Most of the melt inclusions have $(Cl/OH)_m < 0.05$ as a result of high H_2O concentrations (>2 wt%, Fig. 7a); strong changes in $(Cl/OH)_m$ due to degassing therefore do not occur until very low pressures.

7. MODELLING DEGASSING RECORDED BY MELT INCLUSIONS

The distribution of Cl, H_2O and other volatiles (e.g. CO_2) between the melt and co-existing fluid varies depending on the composition of the melt, the pressure, and the fluid–melt distribution coefficient, $D^{fl\text{-}m}$. Once the melt is saturated in volatiles, ascent or crystallisation results in exsolution of a fluid phase. For halogens, $D^{fl\text{-}m} > 1$ so exsolution of H_2O results in halogens being extracted from the melt (e.g. Kilinc and Burnham, 1972; Webster and Holloway, 1988; Shinohara et al., 1989; Webster, 1992; Kravchuk and Keppler, 1994). However, the resulting behaviour of the fluid phase depends on whether the system is closed or open to volatiles (i.e. whether the exsolving fluid phase remains with the melt or can escape the system), how much crystallisation takes place during degassing (Villemant and Boudon, 1999; Edmonds et al., 2001; Harford et al., 2003; Villemant et al., 2008), the extent of re-equilibration between fluid and melt during ascent (e.g. Burgisser and Scaillet, 2007), and whether a brine phase exsolves (e.g. Shinohara et al., 1989; Webster, 1997). Villemant et al. (2008) summarised open-system and closed-system behaviour, and gave the following relationships:

For a closed system (fluid remains with the magma) with no crystallisation:

$$x_i = x_i^0 / [1 + D_i^{fl-m}(X^0_{H_2O} - X_{H_2O})] \quad (3)$$

where i is an element partitioned between melt (m) and fluid (fl), D is the partition coefficient, X is the mass fraction of H_2O in the melt (superscript '0' denotes initial contents) and x_i is the concentration of i in the melt (ppm).

For an open system where there is no crystallisation in the melt:

$$x_i = x_i^0 f^{\delta_i} \quad (4)$$

where $f = 1 - (X^0_{H_2O} - X_{H_2O})$, $\delta_i = D_i^{fl\text{-}m} - 1$ and the fraction of exsolved fluid is 1-f.

For an open system where crystallisation occurs in response to exsolution of H_2O from the melt:

$$x_i = x_i^0 F^{\Delta_i} \quad (5)$$

where $F \approx 1 - (X^0_{H_2O} - X_{H_2O})(1 + k_{m-fl})$, $\Delta i = (D_i{}^{fl-m}/(1 + k_{m-fl})) - 1$, $k_{m\text{-}fl}$ is the mass ratio of crystallising melt to exsolving vapour, and F is the mass fraction of residual melt. In addition, based on experimental data, an exponential dependence of $D_i^{fl\text{-}m}$ is assumed for open-system degassing (Villemant et al., 2008), so that:

$$D_i^{fl-m} = D_0 \exp(K x^m_{Cl}) \quad (6)$$

where K is a constant whose value is $\sim 10^{-3}$–10^{-4} (Villemant et al., 2008).

Because $D_{Cl}^{fl\text{-}m} > 1$, closed-system degassing of H_2O results in a decrease in the melt Cl concentration as Cl is partitioned preferentially into the fluid. Previous studies have typically used relatively high $D_{Cl}^{fl\text{-}m} \sim 10$–$20$ derived from experimental studies (Webster, 1992; Shinohara et al., 1989) although there is some evidence that $D_{Cl}^{fl\text{-}m}$ decreases with pressure (Shinohara et al., 1989; Webster, 1992; Edmonds et al., 2002). In this study we tried a range of $D_{Cl}^{fl\text{-}m}$ from 5–30, with initial melt composition $X^0_{H_2O}$ = 6.4 wt% and Cl = 4500 ppm, estimated on the basis of melt inclusion compositions.

We attempted to fit the melt inclusion compositions using the closed-system degassing (CSD, eq. [4]) or open-system degassing (OSD, eq. [6]) models, and using $D_{Cl}^{fl\text{-}m} \sim$ 5–30 (CSD) or $D_0 \sim 15$–20 (OSD). For H_2O-rich rhyolites $k_{m\text{-}fl}$ is relatively large, and should increase as crystallisation and degassing continue (Villemant et al., 2003, 2008), but its absolute value will depend on eruption dynamics; $k_{m\text{-}fl}$ was observed to be approximately constant during isothermal decompression simulations (Villemant et al., 2003). For OSD we therefore used a constant value of $k_{m\text{-}fl} = 12$ as determined from experimental decompression data (Villemant et al., 2008), consistent with the relatively rapid ascent rate of the January 2007 eruption. For the open-system degassing model, the visually closest fit to the data is given when D_0 is between 5 and 25 with $K \sim 2 \times 10^{-4}$–4×10^{-4}, whereas for closed-system degassing, a range of $D_{Cl}^{fl\text{-}m}$ from 5–30 can fit the data (Fig. 7). This set of values is not unique but represents an envelope of possible values that give fits that enclose the data. The exponential form of $D_{Cl}^{fl\text{-}m}$ from equation [6] results in a variation from $D_{Cl}^{fl\text{-}m} \sim 75$ at 6.5 wt% H_2O to $D_{Cl}^{fl\text{-}m} \sim 25$ for the fully degassed magma, assuming $D_0 = 15$. The main effect of increasing $D_{Cl}^{fl\text{-}m}$ is to decrease the pressure at which the rapid change in $(Cl/OH)_m$ is observed, and to increase $(Cl/OH)_m$ at low pressure (Fig. 7a,b). The differences between the two models are relatively small for the parameters used; however there are differences in the fluid composition produced (Fig. 7d). There is only one previously published measurement of the H_2O/Cl mass ratio in the gas. Gas

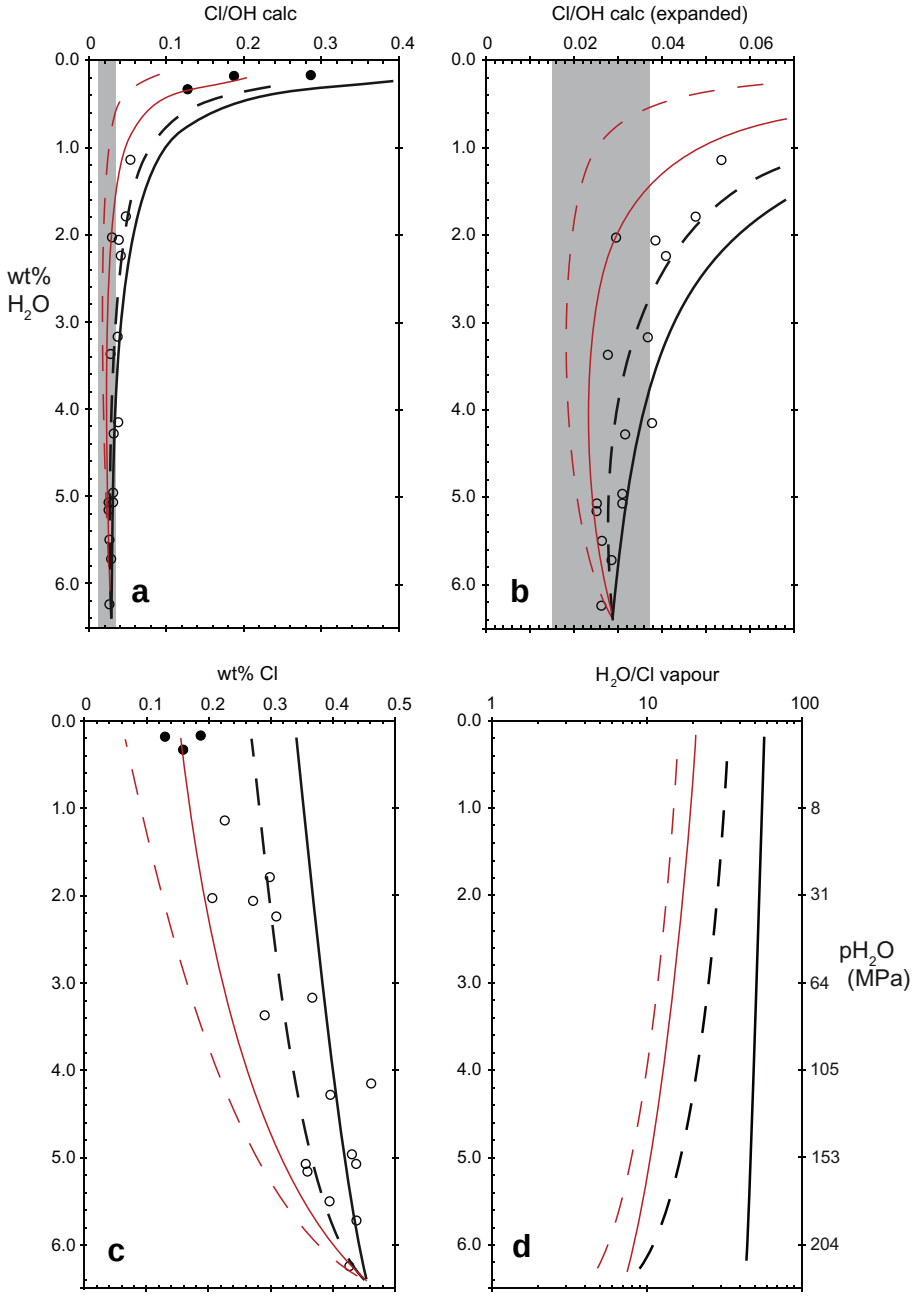

Fig. 7. Results of Cl-H_2O degassing models as a function of melt H_2O content. Open circles are melt inclusions, black circles are matrix glass compositions. Solid lines: closed-system degassing. Dashed lines: open-system degassing accompanied by crystallisation. Thin red lines indicate $D_{Cl}^{fl\text{-}m} = 30$ (CSD) or $D_0 = 25$ (OSD), bold black lines indicate $D_{Cl}^{fl\text{-}m} = 5$ (CSD) or $D_0 = 5$ (OSD). (a) $(Cl/OH)_m$ calculated for the melt, with expanded scale in (b). Grey box indicates the range of $(Cl/OH)_m$ calculated from hornblende compositions. (c) H_2O *vs* wt% Cl. (d) Calculated H_2O/Cl ratio in the exsolved vapour.

was measured from the lava dome in 1996 and gave a value of $H_2O/Cl = 2.9$ (Hammouya et al., 1998). This is lower than predicted by the OSD or CSD models (Fig. 7d), possibly as a result of the very high H_2O contents of this explosive event compared with previous dome rocks, or perhaps precipitation of a brine phase within the fluid during ascent (e.g. Shmulovich and Churakov, 1998; Webster and Mandeville, 2007).

8. ORIGIN OF HORNBLENDE ZONING

The mafic amphiboles are compositionally very distinct from the phenocrysts in the andesite, primarily in that they lack the clear negative correlation between Mg^{vi} and Al^{T}, and have low Cl contents, presumably reflecting a low Cl content in the mafic magma entering the system. However, although the zoning in the phenocrysts shows a decrease in

Cl content at each resorption event, this is not likely to be related to recharge by a low Cl, mafic magma, because the phenocryst compositions do not adjust towards the high Mg^{vi}–Al^{T} composition of the mafic hornblendes (see Fig. 2). Based on the compositional data, the rim zonation also appears to be associated with a decrease in temperature; this is the opposite of what would be expected during magma recharge. More likely causes of zonation involve variations in the volatile composition of the melt and coexisting fluid, including degassing, gas fluxing or convective movements. In the following sections we investigate the result of changes to the volatile content of the melt phase by: (i) degassing processes, (ii) convection and (iii) CO_2 fluxing.

8.1. Degassing processes

The range of $(Cl/OH)_m$ found in the melt inclusions, and predicted by the degassing model (Fig. 7), agree well with the $(Cl/OH)_m$ predicted by hornblende compositions and the partitioning model of Sato et al. (2005). The highest value of $(Cl/OH)_m$ calculated from hornblende compositions is 0.038, consistent with crystallisation from a magma with $\geqslant$2 wt% H_2O according to the melt inclusion compositions ($pH_2O \sim 30$ MPa). This is considerably lower than with the known stability limit of hornblende in H_2O-saturated silicic melt (e.g. ~100 MPa at 800–900 °C, Rutherford et al., 1985; Blundy and Cashman, 2001; ~75 MPa at 850 °C, Holtz et al., 2005). Closed-system exsolution of H_2O from the melt to the vapour phase will result in decreasing H_2O and increasing $(Cl/OH)_m$, while OSD could result initially in a small decrease in $(Cl/OH)_m$, dependent on the amount of concurrent crystallisation and the value of $D_{Cl}^{fl\text{-}m}$ (Fig. 7b). However, even for OSD, a very large fraction of gas, and wide pressure variations (of the order 100 MPa or more) would be required to achieve the necessary decrease in $(Cl/OH)_m$ predicted by the hornblende zoning (c.f. Sato et al., 2005). We therefore conclude that degassing processes alone cannot explain the observed repetitive hornblende zoning.

8.2. Magma convection

Convection in silicic magma chambers has been predicted in numerous studies (e.g. Turner and Campbell, 1986; Martin et al., 1987; Jellinek and Kerr, 1999). Couch et al. (2001) considered convection to be likely at the Soufrière Hills Volcano, on the basis of estimates of the thermal Rayleigh number, which suggested that the critical Rayleigh number will be exceeded for a heated boundary layer greater than a few metres thick. Injection of mafic material could provide the heat source necessary for the formation of a thermal boundary layer near the base of the chamber (Couch et al., 2001). Convection could also provide an explanation for the cyclic nature of the zoning, and the inferred temperature changes.

Because of heat loss from the walls, the magma storage region is likely to be zoned in terms of temperature, crystallinity and gas content, which means that a convecting parcel of material could experience a range of conditions, from cool temperatures and low dissolved volatile contents near the margins, to warmer temperatures and higher dissolved volatile contents (less exsolved vapour) in the interior of the chamber (Fig. 8). We calculated the variation of $(Cl/OH)_m$ as a function of temperature, pressure and crystallinity, to see whether the observed range of $(Cl/OH)_m$ could be produced in a zoned magma chamber. H_2O solubilities in the melt were calculated using the expression of Tamic et al. (2001) for a fluid with $X_{H_2O}^{fl} = 1$ (i.e. $pH_2O = P_{tot}$, no CO_2 present). The crystallinity of the magma was estimated as a function of T and P using an approximation based on published experimental studies of intermediate magma compositions (Blundy and Cashman, 2008):

$$\text{Crystal fraction} = \frac{325 - P}{1000} + \frac{900 - T}{300} \quad (7)$$

where P is in MPa, and T is in °C. For the range of conditions studied (pressures between 160 and 220 MPa and temperatures of 775–875 °C), equation [7] gives reasonable crystallinities of 20–50%, consistent with the observed phenocryst contents (e.g. Murphy et al., 2000).

The dissolved Cl content of a melt with initial composition $X_{H_2O}^{0} = 6.4$ wt% H_2O and $Cl_0 = 4000$ ppm was calculated assuming closed-system degassing with an intermediate partition coefficient ($D_{Cl}^{fl\text{-}m} = 15$, c.f. Fig. 7), incorporating the effects of crystallisation as described in Edmonds et al. (2002):

$$Cl_m = \frac{Cl_0}{f[1 + D_{Cl}^{fl-m}(X_{H_2O}^{0} - X_{H_2O})]} \quad (8)$$

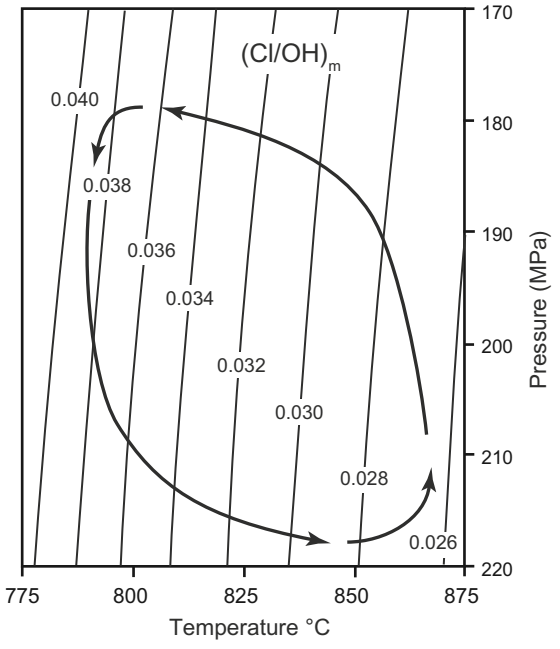

Fig. 8. Contours of $(Cl/OH)_m$ composition as a function of pressure and temperature, at a range of conditions likely to be present within the magma chamber at Soufrière Hills. Curved arrow segments schematically represent the passage of a convecting magma parcel in P-T space. See text for details.

In the zoned system, crystallinity increases with decreasing temperature and melt H_2O content. Cl_m increases slightly with decreasing pressure but strongly with decreasing temperature due to the increase in crystallinity. The calculated variation of $(Cl/OH)_m$ with pressure and temperature is shown in Fig. 8. Similar calculations were also performed for $X^{fl}_{H_2O} = 0.8$. The results are similar, the difference being slightly higher $(Cl/OH)_m$ values as a result of lower H_2O concentrations in the melt.

The calculated $(Cl/OH)_m$ are in agreement with the higher estimates from hornblende compositions, but the lowest hornblende values (~0.02) are not reproduced. However, Fig. 8 illustrates that the positive correlation of $(Cl/OH)_m$ with temperature, inferred from hornblende compositions, cannot be produced by plausible convective motions. Hot material will rise towards the upper parts of the chamber, experiencing decreasing pressure and cooling. Lateral motion towards the chamber walls would result in strong crystallisation with increasing $(Cl/OH)_m$ but decreasing T, with little change in pressure. Downward motion parallel to the walls would result in increasing pressure and temperature, and therefore resorption (Fig. 8). Thus although convective motion could induce the required zoning of $(Cl/OH)_m$, the temperature changes accompanying it would be the opposite of those inferred from hornblende compositions. We therefore reject this explanation.

8.3. CO_2 influx from external source

Another possible explanation for the changes in melt (Cl/OH) ratio is influx of CO_2-rich vapour, perhaps due to degassing of more mafic magma at depth. The effect of this on the melt volatile composition depends on the partitioning behaviour of the mixed H_2O–Cl–CO_2 fluid.

The solubility of Cl and H_2O in rhyolite melt has been examined in several previous experimental studies. At low pressures, an immiscible brine and vapour forms from the fluid at a given Cl_m concentration, at which point Cl_{fl} increases with no change in Cl_m (see Fig. 3, Lowenstern, 2000). For simplicity, this point will be referred to as the Cl solubility limit. At higher pressures (e.g. 200 MPa, depending on the melt composition), a brine phase does not form but mixing remains strongly non-ideal (Shinohara et al., 1989; Carroll and Webster, 1994; Lowenstern, 2000; Webster et al., 1999). At higher pressures, the non-ideality of mixing is reduced (Shinohara et al., 1989). Webster and Holloway (1988) and Metrich and Rutherford (1992) measured a maximum Cl concentration in rhyolite melt at ~0.28 wt%, which occurred with approximately 14 wt% Cl in the coexisting fluid. The Cl solubility limit also depends on composition, increasing with molar (Al + Na + Ca + Mg)/Si ratio (ANCM/S) of the melt and with (Na + K)/Al (Metrich and Rutherford, 1992; Webster, 1997; Webster et al., 1999). The Cl solubility limit increases slightly with increasing temperature and with decreasing pressure (Metrich and Rutherford, 1992; Webster, 1997).

More recent experimental studies for Mount Unzen and Soufrière Hills melt compositions at 200 MPa give a solubility limit of ~0.7–0.8 wt% Cl (Botcharnikov et al., 2004) or ~0.65 wt% Cl (Signorelli and Carroll, 2001) depending on the composition of the melt (e.g. Webster, 1997). This indicates that very high melt Cl concentrations are possible. The melt inclusions analysed in this study typically contain <0.45 wt% Cl (one has 0.55 wt% Cl) so we assume that the Soufrière Hills magma is well below the Cl solubility limit. The inclusions contain up to 6.2 wt% H_2O, equivalent to a pressure of ~215 MPa, or approximately 245 MPa if only 200 ppm CO_2 were present (Newman & Lowenstern 2002).

There is very little experimental data on the behaviour of mixed H_2O–Cl–CO_2 fluids in evolved magmas. However, previous studies show that addition of CO_2 to the H_2O–Cl system causes an expansion of the immiscibility region where vapour and brine coexist (e.g. Joyce and Holloway, 1993; Shmulovich and Graham, 1999; Lowenstern, 2000; Botcharnikov et al., 2007), and the size of this field increases with increasing temperature (Joyce and Holloway, 1993). For relatively Cl-poor fluids, addition of CO_2 lowers the H_2O fugacity of the fluid, leading to decreased H_2O_m (e.g. Botcharnikov et al., 2007); however there is little effect on the Cl content of the melt (Botcharnikov et al., 2007). For Cl-rich fluids, the activities of H_2O and Cl are increased, leading to lower $D_{Cl}^{fl\text{-}m}$ and higher Cl concentrations in the melt (Webster & Holloway 1988; Botcharnikov et al., 2007). Therefore, addition of CO_2 to the andesite magma, perhaps due to degassing of more mafic magma at depth, is a plausible mechanism for increasing (Cl/OH) in the melt, either by reducing [OH] or by increasing Cl_m.

On the basis of these observations, we suggest that CO_2-bearing vapour passes into the andesite as a result of basalt injection near the base of the magma chamber. In the andesite, CO_2 addition results in increasing $(Cl/OH)_m$, and the observed temperature increase results from heat transfer by the gas phase. This has previously been proposed for Soufrière Hills Volcano (e.g. gas sparging, Bachmann and Bergantz, 2003). The effects of CO_2 addition on the crystallising phases are unclear, but experiments run at controlled H_2O–CO_2 fluid composition suggest that a dilution of the fluid by CO_2 at constant temperature can result in decreased modal abundance of hornblende (compared with plagioclase) as well as an increase in total crystallinity (Costa et al., 2004). Therefore accumulation of CO_2 in the magma could eventually result in resorption of hornblende, although heating by the gas phase would also cause resorption as observed at the outer margin of each zone.

On the basis of $(Na + K)^A$ composition, each new hornblende zone starts at lower temperature than that at which resorption occurred. In addition, (Cl/OH) ratios return to approximately their original values and crystallisation resumes. This mechanism therefore requires the gas phase to be fractionated from the melt. This is consistent with the observation that high CO_2 emissions are observed during eruptive pauses as well as during active dome growth, suggesting efficient gas–melt segregation at depth (Edmonds et al., 2008). It is possible that periods of eruption create permeable pathways along which gas can migrate to the surface, while gas accumulates in the magma during periods of repose. The suggestion that transfer of gas from mafic magma into the andesite is supported by the highly

vesicular nature of the mafic inclusions, which formed during quenching against the andesite. Bubbly plumes containing vapour and residual melt may propagate from the mafic-felsic interface during quenching (e.g. Bacon, 1986; Phillips and Woods, 2002).

Extension of the model to include the effects of SO_2 in mixed H_2O–CO_2–Cl–SO_2 fluids is beyond the scope of this study, but it is likely that the mafic magma would also contribute SO_2 gas to the andesite. Experimental work suggests that SO_2 increases $D_{Cl}^{fl\text{-}m}$ (Webster and Holloway, 1988; Botcharnikov et al., 2004; Webster et al., 2009), in contrast to CO_2, but there is a lack of data for H_2O–CO_2–Cl–SO_2 fluids. We recognise the need for further experimental work in order to constrain a multi-component degassing model for intermediate magma compositions. Further melt inclusion work (in progress) will also attempt to quantify CO_2 concentrations in the melt, in order to provide more constraints on degassing processes.

If gas transfer is the cause of rim zonation in hornblendes from the Soufrière Hills magma, then this has implications for the workings of the magmatic system on Montserrat. Firstly, it suggests that volatile release from the system is not continuous – each zone reflects a single episode of gas accumulation and release from the andesite. This may coincide with episodes of chamber refilling by mafic material, and release during eruption. Secondly, the volatile transfer mechanism provides a means of reheating the magma shortly before eruption. Reheating has been inferred for Soufrière Hills on the basis of reversed mineral compositions (e.g. Murphy et al., 2000) and Ti-rich diffusional margins of oxide grains (Devine et al., 2003). The transfer of hot gas from mafic to silicic material is consistent with models of gas sparging, by which relatively immobile, mushy material is rejuvenated prior to eruption (e.g. Bachmann and Bergantz, 2003). Finally, efficient gas–melt segregation at depth would mean that the source of CO_2 measured at the surface includes the mafic part of the system, as previously described for SO_2. Surface gas ratios and concentrations therefore do not provide simple information about degassing of the andesite.

9. CONCLUSIONS

Zoned hornblende phenocrysts from Soufrière Hills Volcano, Montserrat crystallised in a melt that experienced variations in Cl/OH ratio together with temperature changes. The range of $(Cl/OH)_m$ ratios calculated from hornblende compositions is consistent with $(Cl/OH)_m$ calculated from the compositions of plagioclase-hosted melt inclusions in pumice blocks erupted on January 8th 2007. The melt inclusions contain high volatile contents, including up to 6.2 wt% H_2O and 0.44 wt% Cl, implying maximum storage pressures $\geqslant$220 MPa. The data can be described by a closed-system degassing model, or by open-system degassing with a small amount of crystallisation accompanying exsolution. However, the changes in $(Cl/OH)_m$ during decompression and degassing cannot easily explain the Cl zoning in the hornblende phenocrysts. The zoning is consistent with the effects of accumulation of a hot, CO_2-rich volatile phase in the andesite, following injection of mafic magma into the chamber. The significant Cl content of the Soufrière Hills magma, which is at the upper end of the range for arc volcanoes in general, means that a multi-phase volatile model, incorporating the effects of Cl and CO_2, would give the best estimates of pressure from melt volatile contents.

ACKNOWLEDGMENTS

We are grateful for constructive and helpful comments from Roman Botcharnikov, Michael Rowe and an anonymous reviewer, as well as editorial comments from Kelly Russell, which greatly improved the paper. Chiara Petrone is thanked for assistance with electron microprobe analysis. Richard Hinton and the staff of the NERC Ion Microprobe Facility are thanked for their ongoing support and assistance with SIMS analysis. MCSH is supported by a Junior Research Fellowship from Trinity College, Cambridge.

APPENDIX A. SUPPLEMENTARY DATA

Supplementary data associated with this article can be found, in the online version, at doi:10.1016/j.gca.2009.06.014.

REFERENCES

Bachmann O. and Dungan M. A. (2002) Temperature-induced Al-zoning in hornblendes of the Fish Canyon magma, Colorado. *Am. Mineral.* **87**, 1062–1076.

Bachmann O. and Bergantz G. W. (2003) Rejuvenation of the Fish Canyon magma body: a window into the evolution of large-volume silicic magma systems. *Geology* **31**, 789–792.

Bacon C. R. (1986) Magmatic inclusions in silicic and intermediate volcanic rocks. *J. Geophys. Res.* **91**, 6091–6112.

Bacon C. R., Newman S. and Stolper E. (1992) Water, CO_2, Cl, and F in melt inclusions in phenocrysts from three Holocene explosive eruptions, Crater Lake, Oregon. *Am. Mineral.* **77**, 1021–1030.

Barclay J., Rutherford M. J., Carroll M. R., Murphy M. D., Devine J. D., Gardner J. and Sparks R. S. J. (1998) Experimental phase equilibria constraints on pre-eruptive storage conditions of the Soufrière Hills magma. *Geophys. Res. Lett.* **25**, 3437–3440.

Blundy J. and Cashman K. (2001) Ascent-driven crystallisation of dacite magmas at Mount St. Helens, 1980–1986. *Contrib. Mineral. Petrol.* **140**, 631–650.

Blundy J. and Cashman K. (2005) Rapid decompression-driven crystallization recorded by melt inclusions from Mount St. Helens Volcano. *Geology* **33**, 793–796.

Blundy J. and Cashman K. (2008) Petrologic reconstruction of magmatic system variables and processes. *Rev. Mineral. Geochem.* **69**, 179–239.

Blundy J., Cashman K. V. and Berlo K. (2008) Evolving magma storage conditions beneath Mount St. Helens inferred from chemical variations in melt inclusions from the 1980–1986 and current (2004–2006) eruptions. *US Geol. Surv. Prof. Pap.* **1750**, 755–790.

Botcharnikov R. E., Behrens H., Holtz F., Koepke J. and Sato H. (2004) Sulfur and chlorine solubility in Mt. Unzen rhyodacitic melt at 850 C and 200 MPa. *Chem. Geol.* **213**, 207–225.

Botcharnikov R. E., Holtz F. and Behrens H. (2007) The effect of CO_2 on the solubility of H_2O–Cl fluids in andesitic melt. *Eur. J. Mineral.* **19**, 671–680.

Browne B. L. and Gardner J. E. (2006) The influence of magma ascent path on the texture, mineralogy and formation of hornblende reaction rims. *Earth Planet. Sci. Lett.* **246**, 161–176.

Buckley V. J. E., Sparks R. S. J. and Wood B. J. (2006) Hornblende dehydration reactions during magma ascent at Soufrière Hills Volcano, Montserrat. *Contrib. Mineral. Petrol.* **151**, 121–140.

Burgisser A. and Scaillet B. (2007) Redox evolution of a degassing magma rising to the surface. *Nature* **445**, 194–197.

Carroll M. R. and Webster J. D. (1994) Solubilities of sulfur, noble gases, nitrogen, chlorine, and fluorine in magmas. *Rev. Mineral. Geochem.* **30**, 231–279.

Costa F., Scaillet B. and Pichavant M. (2004) Petrological and experimental constraints on the pre-eruption conditions of Holocene dacite from Volcán San Pedro (36 S, Chilean Andes) and the importance of sulphur in silicic subduction-related magmas. *J. Petrol.* **45**, 855–881.

Couch S., Sparks R. S. J. and Carroll M. R. (2001) Mineral disequilibrium in lavas explained by convective self-mixing in open magma chambers. *Nature* **411**, 1037–1039.

Couch S., Sparks R. S. J. and Carroll M. R. (2003) The kinetics of degassing-induced crystallization at Soufrière Hills Volcano, Montserrat. *J. Petrol.* **44**, 1477–1502.

Devine J. D., Gardner J. E., Brack H. P., Layne G. D. and Rutherford M. J. (1995) Comparison of microanalytical methods for estimating H_2O contents of silicic volcanic glasses. *Am. Mineral.* **80**, 319–328.

Devine J. D., Murphy M. D., Rutherford M. J., Barclay J., Sparks R. S. J., Carroll M. R., Young S. R. and Gardner J. E. (1998) Petrological evidence for pre-eruptive pressure–temperature conditions, and recent reheating, of andesitic magma erupting at the Soufrière Hills Volcano, Montserrat. *W.I. Geophys. Res. Lett.* **25**, 3669–3672.

Devine J. D., Rutherford M. J., Norton G. E. and Young S. R. (2003) Magma storage region processes inferred from geochemistry of Fe–Ti oxides in andesitic magma, Soufrière Hills Volcano, Montserrat. *W.I.J. Petrol.* **44**, 1375–1400.

Edmonds M., Pyle D. and Oppenheimer C. (2001) A model for degassing at the Soufrière Hills Volcano, Montserrat, West Indies, based on geochemical data. *Earth Planet. Sci. Lett.* **186**, 159–173.

Edmonds M., Pyle D. and Oppenheimer C. (2002) HCl emissions at Soufrière Hills Volcano, Montserrat, West Indies, during a second phase of dome building: November 1999 to October 2000. *Bull. Volcanol.* **64**, 21–30.

Edmonds, M., Aiuppa, A., Humphreys, M., Giudice, G., Herd, R., Martin, R., Christopher, T., Barclay, J., & Strutt, M. (2008) Bulk volatile concentration in the Soufrière Hills Volcano magma prior to eruption. *IAVCEI 2008 General Assembly,* Iceland, 1-j P06 (abstr.).

Garcia M. O. and Jacobson S. S. (1979) Crystal clots, amphibole fractionation and the evolution of calc-alkaline magmas. *Contrib. Mineral. Petrol.* **69**, 319–327.

Gurenko A. A., Trumbull R. B., Thomas R. and Lindsay J. M. (2005) A melt inclusion record of volatiles, trace elements and Li-B isotope variations in a single magma system from the Plat Pays volcanic complex, Dominica, Lesser Antilles. *J. Petrol.* **46**, 2495–2526.

Hammouya P., Allard P., Jean-Baptiste P., Parello F., Semet M. P. and Young S. (1998) Pre- and syn-eruptive chemistry of gas emissions from Soufrière Hills, Montserrat. *Geophys. Res. Lett.* **25**, 3685–3688.

Harford C. L., Sparks R. S. J. and Fallick A. E. (2003) Degassing at the Soufrière Hills Volcano, Montserrat, recorded in matrix glass compositions. *J. Petrol.* **44**, 1508–1523.

Holland T. and Blundy J. D. (1994) Non-ideal interactions in calcic amphiboles and their bearing on amphibole-plagioclase thermometry. *Contrib. Mineral. Petrol.* **116**, 443–447.

Holtz F., Sato H., Lewis J., Behrens H. and Nakada S. (2005) Experimental petrology of the 1991–1995 Unzen dacite, Japan. Part I: phase relations, phase composition and pre-eruptive conditions. *J. Petrol.* **46**, 319–337.

Humphreys M. C. S., Kearns S. L. and Blundy J. D. (2006) SIMS investigation of electron-beam damage to hydrous, rhyolitic glasses: implications for melt inclusion analysis. *Am. Mineral.* **91**, 667–679.

Humphreys M. C. S., Blundy J. D. and Sparks R. S. J. (2008) Shallow-level decompression crystallisation and deep magma supply at Shiveluch Volcano. *Contrib. Mineral. Petrol.* **155**, 45–61.

Humphreys M. C. S., Christopher T. and Hards V. (2009) Microlite transfer by disaggregation of mafic inclusions following magma mixing at Soufrière Hills Volcano, Montserrat. *Contrib. Mineral. Petrol.* **157**, 609–624.

Jellinek A. M. and Kerr R. C. (1999) Mixing and compositional stratification produced by natural convection. 2. Applications to the differentiation of basaltic and silicic magma chambers and komatiite lava flows. *J. Geophys. Res.* **104**, 7203–7218.

Johnson M. C. and Rutherford M. J. (1989) Experimental calibration of the aluminium-in-hornblende geobarometer with application to Long Valley caldera (California) volcanic rocks. *Geology* **17**, 837–841.

Joyce D. B. and Holloway J. R. (1993) An experimental determination of the thermodynamic properties of H_2O–CO_2–NaCl fluids at high pressures and temperatures. *Geochim. Cosmochim. Acta* **57**, 733–746.

Kilinc I. A. and Burnham C. W. (1972) Partitioning of chloride between a silicate melt and coexisting aqueous phase from 2 to 8 kilobars. *Econ. Geol.* **67**, 231–235.

Kravchuk I. F. and Keppler H. (1994) Distribution of chloride between aqueous fluids and felsic melts at 2 kbar and 800 C. *Eur. J. Mineral.* **6**, 913–923.

Leake B. E., Woolley A. R. and Arps C. E. S., et al. (1997) Nomenclature of amphiboles: report of the subcommittee on amphivoes of the International Mineralogical Association, Commission on new minerals and mineral names. *Can. Mineral.* **35**, 219–246.

Lowenstern J. B. (2000) A review of the contrasting behavior of two magmatic volatiles: chlorine and carbon dioxide. *J. Geochem. Explor.* **69–70**, 287–290.

Martin D., Griffiths R. W. and Campbell I. H. (1987) Compositional and thermal convection in magma chambers. *Contrib. Mineral. Petrol.* **96**, 465–475.

Matthews S. J., Jones A. P. and Bristow C. S. (1992) A simple magma-mixing model for sulphur behaviour in calc-alkaline volcanic rocks: mineralogical evidence from Mount Pinatubo 1991 eruption. *J. Geol. Soc. Lond.* **149**, 863–866.

Metrich N. and Rutherford M. J. (1992) Experimental study of chlorine behavior in hydrous silicic melts. *Geochim. Cosmochim. Acta* **56**, 607–616.

Murphy M. D., Sparks R. S. J., Barclay J., Carroll M. R. and Brewer T. S. (2000) Remobilization of andesite magma by intrusion of mafic magma at the Soufrière Hills Volcano, Montserrat, West Indies. *J. Petrol.* **41**, 21–42.

Newman S. and Lowenstern J. B. (2002) Volatile Calc: a silicate melt-H_2O–CO_2 solution model written in Visual Basic for excel. *Comput. Geosci.* **28**, 597–604.

Nowak M. and Behrens H. (2001) Water in rhyolitic magmas: getting a grip on a slippery problem. *Earth Planet. Sci. Lett.* **184**, 515–522.

Oberti R., Ungaretti L., Cannillo E. and Hawthorne F. C. (1993) The mechanism of Cl incorporation in amphibole. *Am. Mineral.* **78**, 746–752.

Oppenheimer C., Francis P. and Maciejewski J. H. (1998) Spectroscopic observation of HCl degassing from Soufrière Hills Volcano, Montserrat. *Geophys. Res. Lett.* **25**, 3689–3692.

Oppenheimer C., Edmonds M., Francis P. W. and Burton M. (2002) Variation in HCl/SO_2 gas ratios observed by Fourier transform spectroscopy at Soufrière Hills Volcano, Montserrat. In *The eruption of Soufrière Hills Volcano, Montserrat, from 1995–1999*, 21 (eds. T. H. Druitt and B. P. Kokelaar), pp. 21–639. The eruption of Soufrière Hills Volcano, Montserrat, from 1995–1999. Geological Society, London, Memoirs.

Phillips J. C. and Woods A. W. (2002) Suppression of large-scale magma mixing by melt-volatile separation. *Earth Planet. Sci. Lett.* **204**, 47–60.

Plechov P. Yu., Fomin I. S., Melnik O. E. and Gorokhova N. V. (2008) Evolution of melt composition during intrusion of basalts into a silicic magma chamber. *Moscow Univ. Geol. Bull.* **63**, 247–257.

Roman D. C., Cashman K. V., Gardner C. A., Wallace P. J. and Donovan J. J. (2006) Storage and interaction of compositionally heterogeneous magmas from the 1986 eruption of Augustine Volcano, Alaska. *Bull. Volcanol.* **68**, 240–254.

Rowe M. C., Kent A. J. R. and Thornber C. R. (2008) Using amphibole phenocrysts to track vapor transfer during magma crystallization and transport: an example from Mount St. Helens, Washington.. *J. Volcanol. Geotherm. Res.* **178**, 593–607.

Rutherford M. J., Sigurdsson H. and Carey S. (1985) The May 18, 1980 eruption of Mount St. Helens, I. Melt compositions and experimental phase equilibria. *J. Geophys. Res.* **90**, 2929–2947.

Rutherford M. J. and Hill P. M. (1993) Magma ascent rates from amphibole breakdown: an experimental study applied to the 1980-1986 Mount St. Helens eruptions. *J. Geophys. Res.* **98**, 19,667–19,685.

Rutherford M. J. and Devine J. D. (2003) Magmatic conditions and magma ascent as indicated by hornblende phase equilibria and reactions in the 1995–2002 Soufrière Hills magma. *J. Petrol.* **44**, 1433–1454.

Sato H., Nakada S., Fujii T., Nakamura M. and Suzuki-Kamata K. (1999) Groundmass pargasite in the 19991–1995 dacite of Unzen volcano: phase stability experiments and volcanological implications. *J. Volcanol. Geotherm. Res.* **89**, 197–212.

Sato H., Holtz F., Behrens H., Botcharnikov R. and Nakada S. (2005) Experimental petrology of the 1991–1995 Unzen dacite, Japan. Part II: Cl/OH partitioning between hornblende and melt and its implications for the origin of oscillatory zoning of hornblende phenocrysts. *J. Petrol.* **46**, 339–354.

Scaillet B. and Evans B. W. (1999) The 15 June 1991 eruption of Mount Pinatubo. I. Phase equilibria and pre-eruption P-T-fO_2-fH_2O conditions of the dacite magma. *J. Petrol.* **40**, 381–411.

Schumacher J. C. (1997) The estimation of the proportion of ferric iron in the electron-microprobe analysis of amphiboles. *Can. Mineral.* **35**, 238–246.

Shinohara H., Iiyama J. T. and Matsuo S. (1989) Partition of chlorine compounds between silicate melt and hydrothermal solutions: I. Partition of NaCl–KCl.. *Geochim. Cosmochim. Acta* **53**, 2617–2630.

Shmulovich K. I. and Churakov S. V. (1998) Natural fluid phases at high temperatures and low pressures. *J. Geochem. Explor.* **62**, 183–191.

Shmulovich K. I. and Graham C. M. (1999) An experimental study of phase equilibria in the system H_2O-CO_2–NaCl at 800 C and 9 kbar. *Contrib. Mineral. Petrol.* **136**, 247–257.

Signorelli S. and Carroll M. R. (2001) Experimental constraints on the origin o chlorine emissions at the Soufrière Hills Volcano, Montserrat. *Bull. Volcanol.* **62**, 431–440.

Sparks R. S. J., Murphy M. D., Lejeune A. M., Watts R. B., Barclay J. and Young S. R. (2000) Control on the emplacement of the andesite lava dome of the Soufrière Hills Volcano, Montserrat by degassing-induced crystallization. *Terra Nova* **12**, 14–20.

Stix J., Layne G. D. and Williams S. N. (2003) Mechanisms of degassing at Nevado del Ruiz Volcano, Colombia. *J. Geol. Soc. Lond.* **160**, 507–521.

Symonds R. B., Rose W. I., Gerlach T. M., Briggs P. H. and Harmon R. S. (1990) Evaluation of gases, condensates and SO_2 emissions from Augustine Volcano, Alaska: the degassing of a Cl-rich volcanic system. *Bull. Volcanol.* **52**, 355–374.

Tamic N., Behrens H. and Holtz F. (2001) The solubility of H_2O and CO_2 in rhyolitic melts in equilibrium with a mixed CO_2–H_2O fuid phase. *Chem. Geol.* **174**, 333–347.

Turner J. S. and Campbell I. H. (1986) Convection and mixing in magma chambers. *Earth Sci. Rev.* **23**, 255–352.

Villemant B. and Boudon G. (1999) H_2O and halogen (F, Cl, Br) behaviour during shallow magma degassing processes. *Earth Planet. Sci. Lett.* **168**, 271–286.

Villemant B., Boudon G., Nougrigat S., Poteaux S. and Michel A. (2003) Water and halogens in volcanic clasts: tracers of degassing processes during Plinian and dome-building eruptions. In *Volcanic Degassing*, 213 (eds. C. Oppenheimer, D. M. Pyle and J. Barclay). Geological Society of London Special Publication, pp. 3–79.

Villemant B., Mouatt J. and Michel A. (2008) Andesitic magma degassing investigated through H_2O vapour-melt partitioning of halogens at Soufrière Hills Volcano, Montserrat (Lesser Antilles). *Earth Planet. Sci. Lett.* **269**, 212–229.

Volfinger M., Robert J.-L., Vielzeuf D. and Neiva A. M. R. (1985) Structural control of the chlorine content of OH-bearing silicates (mica and amphiboles). *Geochim. Cosmochim. Acta* **49**, 37–48.

Wallace P. J. (2005) Volatiles in subduction zone magmas: concentrations and fluxes based on melt inclusion and volcanic gas data. *J. Volcanol. Geotherm. Res.* **140**, 217–240.

Webster J. D. (1992) Fluid-melt interactions involving Cl-rich granites: experimental study from 2 to 8 kbar. *Geochim. Cosmochim. Acta* **56**, 659–678.

Webster J. D. (1997) Chloride solubility in felsic melts and the role of chloride in magmatic degassing. *J. Petrol.* **38**, 1793–1807.

Webster J. D. and Holloway J. R. (1988) Experimental constraints on the partitioning of Cl between topaz rhyolite melt and H_2O and $H_2O + CO_2$ fluids: new implications for granitic differentiation and ore deposition. *Geochim. Cosmochim. Acta* **52**, 2091–2105.

Webster J. D., Kinzler R. J. and Mathez E. A. (1999) Chloride and water solubility in basalt and andesite melts and implications for magmatic degassing. *Geochim. Cosmochim. Acta* **63**, 729–738.

Webster, J. D., Sintoni, M. F., & De Vivo, B. (2009) The partitioning behavior of Cl, S, and H_2O in aqueous vapor- $\pm$ saline-liquid saturated phonolitic and trachytic melts at 200 MPa. *Chem. Geol*. Available at doi:10.1016/j.chemgeo.2008.10.017.

Webster J. D. and Mandeville C. W. (2007) Fluid immiscibility in volcanic environments. *Rev. Mineral. Geochem.* **65**, 313–362.

Young S. R., Francis P. W., Barclay J., Casadevall T. J., Gardner C. A., Darroux B., Davies M. A., Delmelle P., Norton G. E., Maciejewski A. J. H., Oppenheimer C. M. M., Stix J and Watson I. M. (1998) Monitoring SO_2 emission at the Soufriere

Hills Volcano: implications for changes in eruptive conditions. *Geophys. Res. Lett.* **25**, 3681–3684.

Zellmer G. F., Sparks R. S. J., Hawkesworth C. J. and Wiedenbeck M. (2003) Magma emplacement and remobilization timescales beneath Montserrat: insights from Sr and Ba zonation in plagioclase phenocrysts. *J. Petrol.* **44**, 1413–1431.

Zhang Y. (1999) H_2O in rhyolitic glasses and melts: measurement, speciation, solubility, and diffusion. *Rev. Geophys.* **37**, 493–516.

Associate editor: J.K. Russell